Materials Chemistry and Physics 287 (2022) 126294

Contents lists available at ScienceDirect

Materials Chemistry and Physics

journal homepage: www.elsevier.com/locate/matchemphys

# Chitosan-xanthan gum PEC-based aerogels: A chemically stable PEC in $scCO_2$

Luciana I.N. Tomé, Marco S. Reis, Hermínio C. de Sousa, Mara E.M. Braga *

*University of Coimbra, CIEPQPF, FCTUC, Department of Chemical Engineering, Rua Sílvio Lima, Pólo II - Pinhal de Marrocos, 3030-790, Coimbra, Portugal*

## HIGHLIGHTS

- Chitosan-xanthan gum PEC-based aerogels.
- A chemically stable chitosan-xanthan gum-based PEC in $scCO_2$.
- The aerogel processed at 150 bar shows higher porosity.

## GRAPHICAL ABSTRACT

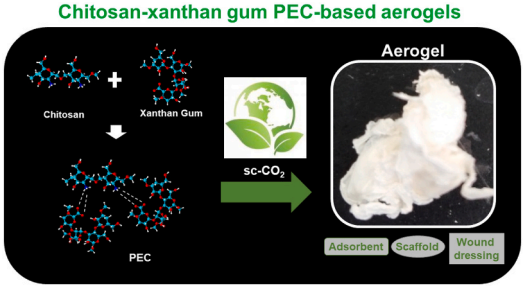


## ARTICLE INFO

*Keywords:*
Polyelectrolyte complexes
Aerogels
DOE
Supercritical-drying
Xanthan gum
Chitosan

## ABSTRACT

An innovative aerogel obtained from a chitosan/xanthan gum polyelectrolyte complex (PEC) was developed in this work from the screening of thirteen different combinations of natural polyelectrolytes: two positively-charged biopolymers (chitosan and gelatin A), six negatively-charged biopolymers (pectin, iota-carrageenan, collagen, xanthan gum, alginate and modified galactomannan), and a neutral polymer (guar gum) using the statistical design of experiments (DOE) approach. Only the chitosan-xanthan gum formed aerogels under supercritical conditions using carbon dioxide at 150 bar and 250 bar and 35 °C. The chitosan-xanthan gum-based aerogels have bone-like structures and smooth surfaces, with pore size distributions in the meso- and macropore ranges, the average pore diameter of ~20 nm and porosity between 60 and 70%. The specific surface areas of the aerogels processed at 150 bar and 250 bar are, respectively, 5.7 and 17.5 $m^2\ g^{-1}$, values below those commonly reported in the literature for aerogels. The aerogels are thermally stable up to ~240 °C, while the cryogel is thermally stable up to ~224 °C. The value of the total weight loss through thermal decomposition of the aerogels (~25%) is smaller than that of the cryogel (~40%). These materials have potential applications in the environmental and biomedical areas, providing solutions to the current challenges in biomedicine and social, demographic and sanitary life sciences.

## 1. Introduction

In the scenario of a circular economy and sustainability, the production of aerogels from natural polymeric materials has shown to be quite convenient and to present an enlarged spectrum of potential applications [1,2]. Natural polymers obtained from renewable sources can

* Corresponding author.
*E-mail address:* marabraga@eq.uc.pt (M.E.M. Braga).

https://doi.org/10.1016/j.matchemphys.2022.126294
Received 7 March 2022; Received in revised form 13 May 2022; Accepted 16 May 2022
Available online 20 May 2022

be used to produce aerogels. The combination of polymers to produce materials with specific characteristics can be interesting and innovative.

Aerogels are nanoporous materials typically characterized by having a high porosity (~80–99.8%), low density (<0.5 g $cm^{-3}$) and large surface area (~500–1200 $m^2$ $g^{-1}$), among other interesting features [3]. Among the numerous types of precursors that can be used to produce aerogels, biopolymers derived from renewable resources have been increasingly considered. Their non-toxic, biocompatible and biodegradable nature has been pointed out as ideal for biomedical applications such as tissue engineering, drug delivery and biosensing [1,4]. Quite often, however, the need for better control of the properties of these materials leads to the use of chemical crosslinkers to improve their usage in different applications. These are usually toxic and difficult to eliminate, compromising the biocompatibility of aerogels, which is undesirable for biomedical applications [5–8]. Among the strategies proposed to avoid this problem [9], the use of polyelectrolyte complexes (PECs) for the fabrication of aerogels has been recognized as a possible solution [1,10,11]. Under adequate conditions, the mixture of oppositely charged biopolymers leads to the formation of PECs, without the interference of (cyto)toxic or harmful chemical cross-linking agents, since they are able to self-crosslink electrostatically. The results are biodegradable, biocompatible and non-toxic materials [11], with the additional advantage of being produced through simple, sustainable, eco-friendly, energy- and cost-efficient processes [12].

The systematic synthesis, pilot-scale production and commercialization of bioaerogels are still giving their first steps [13]. For the development of bioaerogels, a variety of pure polysaccharides such as agar, alginate, cellulose, chitin, chitosan, lignin, pectin, carrageenan, xanthan gum, guar gum, pullulan, lignin and starch, and proteins have been considered and their synthesis approaches, properties and applications extensively reported and reviewed [2,4,5,14–19]. Appropriate combinations of biopolymers have also been shown to display improved properties and enhanced opportunities for biomedical usage of the correspondent aerogel structures [2,5], though the number of papers published is still scarce. For instance, alginate/chitosan-based aerogels have been suggested for wound healing applications [20], pectin/xanthan aerogels for orthopedics applications [21], chitosan-coated pectin aerogels for drug delivery [22], alginate/starch aerogels for bone regeneration [23], cellulose/gelatin for skin regeneration [24] and collagen/alginate [25] as scaffolds for tissue engineering. The use of PECs for the production of aerogels has not actually been the object of intensive research, though unequivocally pointed out as promising [20]. One of the few examples available so far is the case where the aerogel is obtained from stoichiometric alginate-chitosan PEC [20,26].

One of the problems largely faced in the processing of naturally based aerogels is the thermal degradation and/or deformation of pores caused by the pressure produced during supercritical drying. These can theoretically be overcome by the selection of adequate pressure/temperature drying conditions. Alginate-based aerogel materials were shown to maintain nanostructure when $scCO_2$-drying was performed at 150 bar and 38 °C [27]. Both alginate-gelatin and chitosan-gelatin aerogels preserved shape and volume when $scCO_2$-dried at 200 bar and 35 °C, providing aerogels with high porosity [28], though further reticulation with $CaCl_2$ or crosslinking with glutaraldehyde were used, respectively.

In this work, an innovative aerogel was developed from a chitosan/xanthan gum-based PEC, after an exhaustive screening of natural polyelectrolyte combinations. Processing and characterization studies were carried out for the chitosan/xanthan gum aerogel samples. Cryogels were obtained from all the PECs derived from the polyelectrolyte combinations tested. To the best of our current knowledge, there are no publications so far reporting the development and study of the material presented in this research.

## 2. Materials and methods

### 2.1. Materials

Chitosan (CS, medium molecular mass, 75–85% degree of deacetylation), iota-carrageenan (CRG, commercial grade, Type II), pectin from citrus fruits (PT, 74% galacturonic acid), gelatin from porcine skin (GEL, Type A), alginic acid sodium salt from brown algae (ALG, bioreagent), guar gum (GG) and xanthan gum (XG) were purchased from Sigma-Aldrich, Germany. Collagen (COL) was kindly provided by Professor Marta R. Fontanilla from Universidad Nacional de Colombia [29], and galactomannan (GLM) (extracted from Tara, *Caesalpinia spinosa*) fruit seed coat [30]) was acquired from Transformadora Agrícola S.A.C., Brazil.

All reagents were used as received, except collagen and galactomannan which were further modified (see Section 2.2).

Sodium hydroxide PA pellets (EKA/Spoilchemie, Rocara, Ireland) and 2,2,6,6-tetramethylpiperidine-1-oxyl (TEMPO, Sigma-Aldrich, Germany) were used for the modification of the reagents.

The 0.1 M acetate buffer solution pH 4.5 was prepared with glacial acetic acid (Fluka, Switzerland) and sodium acetate 3-hydrate (≥99%, Panreac, Spain).

Distilled water was employed throughout the work.

### 2.2. Preparation of PECs

Deacetylation of CS was performed following the method described by Chang et al. [31]. Commercial CS was dissolved in 60% (m/v) NaOH solution and stirred for 4 h in a constant temperature oil bat at 100 °C. The precipitated polymer was filtered and washed several times with distilled water until the pH of the filtrate reached 7. The final product was dried in a vacuum oven at 50 °C, for 24 h. The deacetylation degree of CS was determined by $^1$H NMR spectroscopy (99.3%) [32] and further confirmed by FTIR analysis (98.7%) [33].

Galactomannan was modified by a selective oxidation process to produce an anionic polyelectrolyte. The oxidation of GLM was carried out using the reagent TEMPO, according to the procedure described by Sierakowski et al. [34]. The maximum degree of oxidation was assured by a 4 h reaction time and the yield of carboxylation confirmed by the amount of NaOH consumed (3.0 mEq per gram of GLM in reaction) [34]. The modified polymer was characterized by FTIR spectroscopy, confirming the presence of carboxylate groups.

Polyelectrolyte solutions 1% (m/v) were prepared in water or in acetate buffer pH 4.5 (CS and PT) or in acetic acid (COL) [35–37]. 0.38% (m/v) CS and 0.63% (m/v) CRG [38], 0.6% (m/v) CS [39] and 1.5% (m/v) XG [40] were additionally prepared.

The pH of the polyelectrolyte starting solutions and of the CS-XG 1.5% prepared was measured at 25 °C, using a Jenway, 3510 pH Meter.

Factors and levels used in the final factorial design for the systems studied are presented in Table 1. Additional information, such as polyelectrolyte combinations and volume of the cationic and of the anionic polyelectrolyte, other tested levels and the conditions defined for each run are presented in Table S1.

Magnetic stirring was carried out in a Unitron MS-52 M multichannel stirrer. Orbital stirring was performed using a JeioTech Infors

**Table 1**
Factors and levels used in the factorial design for the systems studied.

| Factor | Level | |
|---|---|---|
| | High (+) | Low (−) |
| Deacetylation degree[a], % | 98 | 75–85 |
| Type of stirring, rpm | Magnetic (150) | Orbital (50) |
| Vial diameter/$V_{total}$, cm.$ml^{-1}$ | 0.25 | 0.42 |
| m/m (CS), % | 83 | 17 |

[a] For chitosan samples.

HT CH-4103 shaker, and dispersion stirring was executed in IKA-T18 basic Ultra-Turrax.

The PECs were prepared at least twice for each composition.

### 2.3. Screening of natural polyelectrolyte combinations

#### 2.3.1. Statistical design of experiments

In a preliminary exploratory phase carried out with literature support, CS-based systems were used to explore and assess the effectiveness of different experimental conditions. The main contributing factors to the formation of PECs identified in the preliminary test phase were further screened and optimized. For such, two-level fractional factorial designs, with 4 factors for CS-based PECs and 3 factors for the remaining systems were applied (Table S1), and the results were statistically analyzed. As the response is categorical (hydrogel formation), the screening of significant factors was carried out one by one, using: a $\chi^2$ test based on the contingency table for categorical factors; logistic regression for continuous factors. The significance was assessed using the corresponding raw *p*-values and p-values adjusted for controlling false discovery rate (FDR) (implemented in JMP Pro version 16.0.0). All the polyelectrolyte combinations considered in this work were studied and, for each system, the 4 variables were crossed with the response (hydrogel formation), to identify the factors which best explain the distribution between them and the occurrence or not of hydrogel formation. Five factors were screened as significant (Fig. S1), which are represented in Fig. 1.

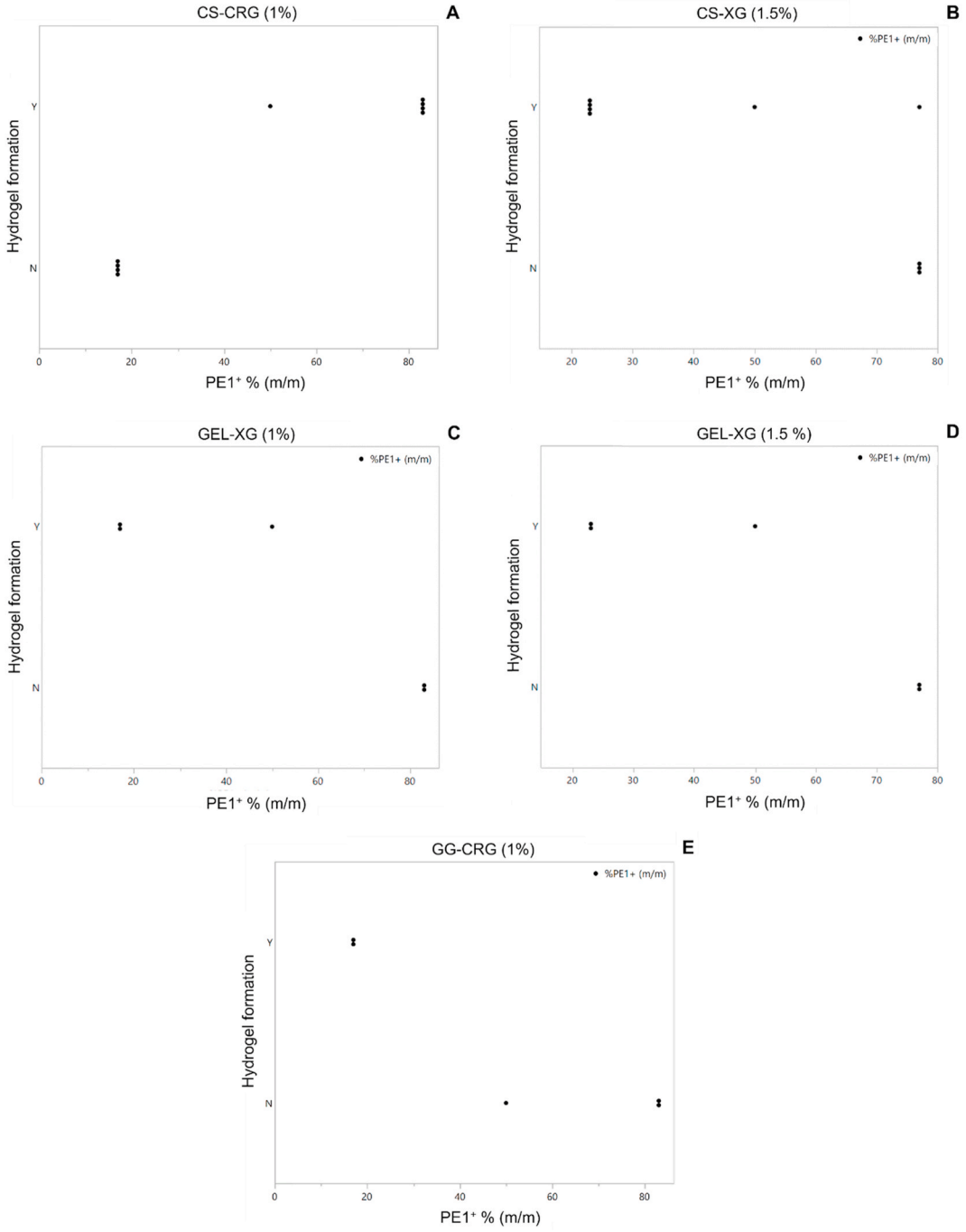


**Fig. 1.** Plots of the response (hydrogel formation) *vs* the main factor (%$PE^+$) for the polyelectrolyte combinations selected.

#### 2.3.2. Confirmation of PEC formation by Fourier transform infrared (FTIR) spectroscopy

The FTIR analysis was performed using an FTIR spectrometer (JascoFT/IR-4200, Japan), operating in ATR mode and potassium bromide disks for the powder samples, in the range 4000–500 $cm^{-1}$, spectral resolution 4 $cm^{-1}$ and 64 scans. Spectra were obtained for the PECs studied, as well as for the pure starting precursors.

### 2.4. Sample processing

The systems for which evidence for PEC formation was obtained were further processed and converted into aerogels or cryogels.

For the production of aerogels, the samples were the first solvent exchanged by successively immersing in ethanol/water mixtures with concentrations of 40% (for 2.5 h), 70% (for 2.5 h) and 100% (for 24 h). Soaking in 100% ethanol was performed twice to guarantee the alcolgel formation.

Then, the alcogels were dried with $scCO_2$. Sc-drying was performed in equipment for supercritical extraction (Separex, France), using a 20 mm diameter cylindric cell with 20 ml capacity. A gas flow meter (Alexander Wright, London, UK) enabled the determination of the volume of $CO_2$ used and the inlet flow rate. The pressure in the cell, and consequently, the output $CO_2$ flow rate was controlled through the manipulation of two valves, one of which is a micrometric valve. An ethylene glycol cooling bath at 3.5 °C was employed as the $CO_2$ cooling system. Drying was performed at 150 bar, 35 °C, flow rate 0.5 ml $min^{-1}$, during 4 h, for all the systems studied.

Among all the combinations tested (Table S1), only the CS-XG PEC provided stable aerogels and was therefore selected for further studies. The remaining systems investigated, either did not form PECs or did not form stable aerogels.

For the CS-XG 1% system, two different pressure values (150 and 250 bar) were considered, maintaining the rest of the experimental drying conditions. The mass of $CO_2$ used per gram of dried polymer was found to be $3 \times 10^{-5}$ kg and $1.7 \times 10^{-5}$ kg for the processing at 150 bar and at 250 bar, respectively.

The hydrogels were frozen at −18 °C and lyophilized under −80 °C and 0.10 mbar for 24 h, using a Telstar LyoQuest Lyophilizer.

At least three replicates were produced for each polymeric system studied.

### 2.5. Physical characterization

The microstructure, morphology and properties of the chitosan-xanthan gum-based aerogels and cryogels (CS-XG 1%) were studied by a variety of techniques.

Density measurements of the materials were carried out using the helium picnometry technique (Micrometrics equipment, model Accupyc 1330).

The specific surface area (BET) and average pore diameter of the cryogels and aerogels were determined by the nitrogen adsorption method (ASAP 2000 Micrometrics equipment, model 20Q-34001-01).

Mercury intrusion porosimetry technique (Micrometrics equipment, model AutoPore IV) was employed to obtain the bulk and skeletal densities, the porosity and the total area of the pores of the dried samples.

The morphology of the cryogels and aerogels was analyzed by scanning electron microscopy (SEM) (Veja3, Tescan equipment). The sample was coated with a 10 nm film of gold and palladium for 30 s and an acceleration voltage of 5 kV. The magnifications used were 100 ×, 5000 × and 25 000 ×.

### 2.6. Thermal analysis

The thermal stability analysis of the CS-XG 1% aerogels and cryogel was carried out using Simultaneous Data Thermal (SDT) analysis (Q600, TA Instruments, USA). Samples (6–10 mg) were analyzed with a heating rate of 10 °C $min^{-1}$ from 25 °C to 600 °C, under nitrogen flow. This analysis was performed in duplicate.

## 3. Results and discussion

### 3.1. Screening of natural polyelectrolytes combinations and chemical stability of PECs in $scCO_2$

The experimental designs used to optimize the parameters, and the responses obtained for the PEC systems studied are given in Table S1. Fig. 1 depicts the corresponding 3D response surface graph.

The formation of PECs was visually detected for eight polyelectrolyte combinations: CS-PT; CS-CRG, CS-XG 1%, CS-XG 1.5%; GG-CRG; GG-XG; GEL-XG 1% and GEL-XG 1.5% (Table S1). Within a given system, not all combinations of parameters derived from DOE led to the production of PECs.

Among the factors studied, the $PE1^+$ content (%, m/m) (and consequently the $PE1^+$:$PE2^-$ ratio) was identified as the major factor controlling the formation of PECs. For each system, the best sample was selected using the hydrogel formation assessment as the criterion (Table S1). The selected samples were further analyzed by FTIR spectroscopy.

After running all the polyelectrolyte combinations tested in this work and crossing the 4 factors with the response (hydrogel formation), 5 cases (Fig. 1) revealing a significant effect of the factor %$PE1^+$ and the hydrogel formation were detected, meaning that the former is the crucial parameter for these systems. When the relationship between this predictor and the response is considered, stronger results are observed for the CS/CRG-based aerogels, showing a clear separation of situations leading to hydrogel formation (Fig. 1A). The second most significant results were found for system CS/XG 1.5% (Fig. 1B), followed by GEL/XG (Fig. 1C) and GEL/XG (Fig. 1D), and finally GG/CRG (Fig. 1E).

The FDR approach was implemented using adjusted p-values for each test (to facilitate the comparison with the target FDR, which in this work was set to 0.05). FDR controls for the false discovery of significant effects in multiple testing problems, such as in the current situation [41]. This is a less conservative approach than controlling for the overall error rate (also known as Family Wise Error Rate, FMWER), which is often too restrictive. Both the FDR and FWER approaches were applied in the present work (see thresholds used in Fig. S1 for selecting the significant effects). As referred above, FDR was controlled at a level alpha of 0.05, to guarantee that the percentage of false positives (null features deemed significant) out of all hypothesis tests is 5% or less. Only the variable % $PE1^+$ was able to explain the hydrogel formation, as can be observed in the plot of FDR adjusted p-values and raw p-values against the rank fraction (Fig. S1). All the points lying below the blue and red lines shown in Fig. 1 are the ones considered significant according to the FDR and FWER criteria.

The selected samples were further analyzed by FTIR spectroscopy. The FTIR data obtained supported the formation of CS-PT, CS-CRG, CS-XG 1% and CS-XG 1.5% PECs. For the other systems, the spectroscopic evidence was not conclusive. Fig. 2 provides the FTIR spectra of the PECs and the corresponding sum spectra, obtained as the weighted sum of the spectra of the individual starting polyelectrolytes. Globally, the PECs spectra show the main changes in the range 1400–1600 $cm^{-1}$, providing evidence for the interaction between the anionic and cationic charged groups of the polymers.

Polyelectrolyte complexes are formed mainly by ionic crosslinking. The pH determines the available free charges of each polyelectrolyte, directly influencing its complexation, as well as the polymer ratios. For the CS-based systems, only 1:5 (v/v) CS/$PE^-$ ratios lead to the formation of PECs (Table S1). It is expected that chitosan interacts with pectin to form PECs through $NH_3^+/COO^-$ charge interactions. At pH 5.26 and 5.15 of the corresponding starting solutions, commercial and deacetylated chitosan are only 0.3% ionized, and 20% of the carboxyl groups of pectin

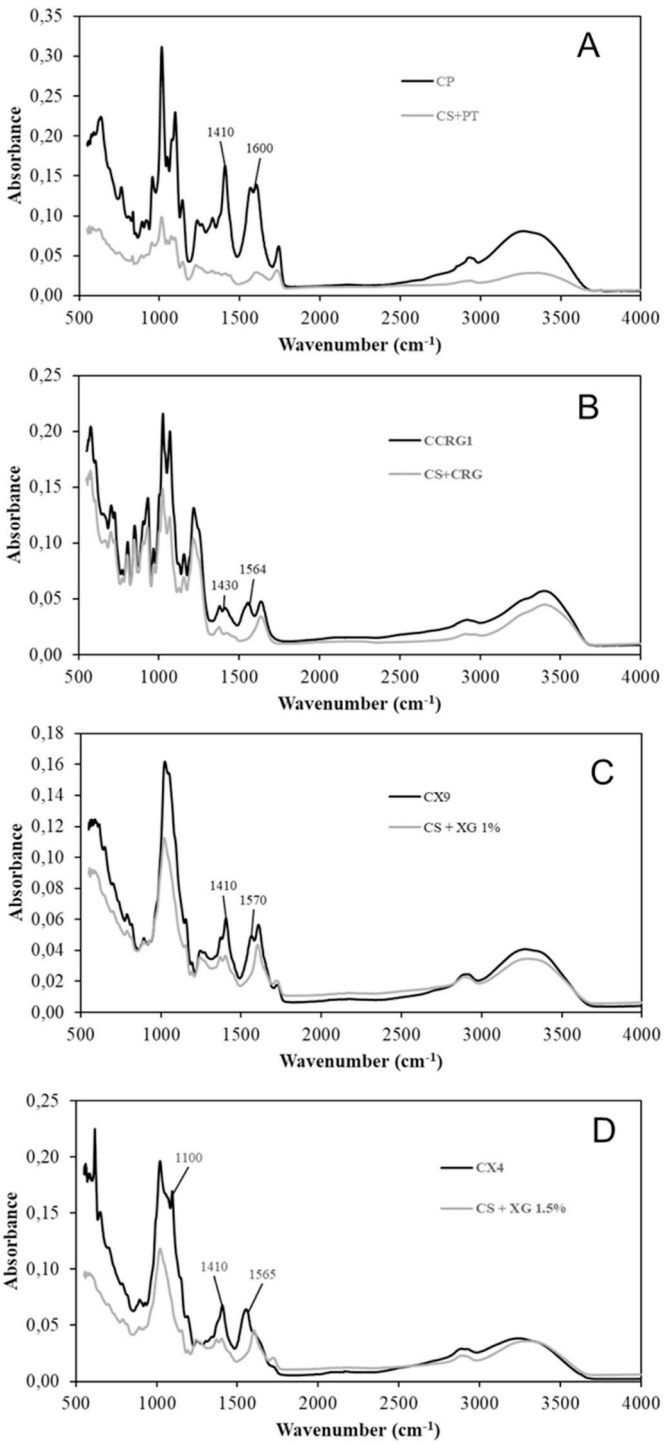


**Fig. 2.** FTIR spectra of CS-PT (CP2) (**A**), CS-CRG (CCRG1) (**B**), CS-XG 1% (CX9) (**C**) and CS-XG 1.5% (CX4) (**D**) PECs, and the corresponding sum spectra.

are in the anionic form at pH 4.12 of the polyelectrolyte starting solution. Considering the 1:5 (v/v) CS/PT PEC, there is a large excess of pectin and therefore, free negative charges inside the polymeric network (in the order of 50 nmol $dm^{-3}$). Lower pectin concentrations do not result in the production of PECs. These data suggest that a low ionic crosslinking density but a high amount of hydrogen bonds due to the anions of pectin increase the crosslinking density of the hydrogel. Furthermore, the absence of free positive amine groups in the chitosan chain leads to reduced repulsion, resulting in more stable hydrogels. Similar arguments are valid to explain CS/XG-based PEC formation. At pH 5.06 of the starting solution, only 0.8% of the carboxyl groups of XG are in the anionic form. When combined with CS in the 1:5 (v/v) CS/XG proportion, an excess of less than 1 nmol $dm^{-3}$ of ionized $COO^-$ groups of XG will be present in the medium, after the interaction with $NH_3^+$. This slight excess of anions confers the opportunity to additionally establish hydrogen bonds, increasing the crosslinking density of the hydrogels. This does not occur for lower XG ratios in the polymers mixtures, and these do not form hydrogels. As far as CS/CRG PECs are concerned, though CRG is only about 0.1% ionized in the $SO_3^-$ form at pH 5.58 of the starting solution, only ~0.03 nmol $dm^{-3}$ of $SO_3^-$ will be in excess at 1:5 (v/v) CS/CRG ratios, and PEC formation is mainly the result of $NH_3^+$/$SO_3^-$ electrostatic interactions. Lower CRG ratios do not result in PEC formation, suggesting that the stabilization of the structure is not reliant on the number of electrostatic interactions, but on lessen to allow broader network formation. Similar arguments have been presented before to explain CS/XG- [42] and CS/CRG- [43] based PECs.

The formation of CS/COL is not observed, independently of the ratio of the polymer. It has been shown that, at room temperature, whatever the conditions, there is always a competition between collagen gelation and the formation of a pure CS/COL polycation/polyanion complex, and thus only a small percentage of the negative $COO^-$ groups of COL which are not involved in the gelation process are available to participate in the PEC [44].

There are polymeric combinations tested that visually form theoretically predictable PECs; nevertheless, no clear evidence from FTIR spectroscopy suggesting PEC formation has been gathered. This is the case of GEL/XG 1.5%, GG/CRG and GG/XG-based matrixes at 1:5 (v/v) ratios and GEL/XG 1% at 1:1 (v/v) proportion.

The amine and carboxyl groups of GEL and XG are, at pH 5.38 and 5.06, 0.1% and 0.8% in their charged forms, respectively. This means that an excess of ~200 nmol $dm^{-3}$ of $NH_3^+$ moieties of GEL will be in the medium, after the $COO^-/NH_3^+$ charge compensation in GEL/XG 1% 1:1 (v/v) PECs. In the case of GEL/XG 1.5%, in the 1:5 (v/v) ratio, this value is very similar. It has been shown that non-coulombic interactions involving NH and OH groups, as well as hydrophobic interactions do also play a role in GEL/XG PEC formation [45]. Steric hindrance of XG is likely to create a certain obstruction in the way that the polymers interact with each other, and that is probably the reason why complexes comprising a higher XG proportion are not observed.

Independently of the polymers ratio considered, GEL/CRG PECs were not obtained in this work. An excess of approximately 200 nmol $dm^{-3}$ of $NH_3^+$ groups would be as well expected; the non-formation of the PEC will thus be related to the structure of CRG which, contrarily to XG, does not have the ability to participate so effectively in hydrogen bonding involving NH and OH groups, since the density of the hydroxyl groups in its polymeric chains is considerably smaller.

GG is a neutral polysaccharide and, when combined with polyelectrolytes, the resulting matrix is not accurately a PEC, according to the definition commonly accepted. Nevertheless, and though uncharged, GG is (theoretically) able to bind to charged polymers through hydrogen bonding as the result of the hydroxyl groups present in the polymeric chains. GG/CRG e GG/XG hydrogels were observed for 1:5 (v/v) proportions, though not confirmed by FTIR evidence, while GG/PR and GG/ALG PECs were not formed. The anionic moiety in CRG is $OSO_3^-$, whereas, in XG, PT and ALG is $COO^-$. Greater polarization of the sulfonate groups, when compared to carboxyl, should provide a stronger ionic association ability. On the other hand, XG possesses more ramifications and a higher OH density than the other polyelectrolytes. These two factors can explain the ability of GG to form (or not) PECs with the polyelectrolytes tested.

No PECs involving modified GLM were observed in this work. Despite being experimentally confirmed, the presence of the carboxylate groups in modified GLM might have not been high enough to confer the polymer the ability to form PECs.

Replicates of the selected samples described in Table S1 were prepared for the systems for which the FTIR evidence corroborated the

successful formation of PECs and converted into aerogels by $scCO_2$-drying or into cryogels. The results are provided in Fig. 3. Only the CS-XG PECs prepared from 1% m/v starting solutions yielded aerogels by $scCO_2$-drying. Using the existence of visual and FTIR evidence for PEC formation and the production of stable aerogels as the criteria, the CS-XG 1% system (and CX9 samples) was selected to be further studied. All the other polyelectrolyte combinations were still alcolgels after drying 5 h with $scCO_2$. On the other hand, cryogels were successfully obtained for all the polyelectrolyte combinations considered.

The reason why it is possible to obtain cryogels and not aerogels for all the samples lies on the reduction in the pH of the medium during sc-drying due to the *in situ* generation of ethylcarbonic acid from $CO_2$ and ethanol. The electrostatic interactions established between functional groups that can be ionized or protonated are pH-dependent. As far as the systems under study are concerned, those interactions occur between $NH_3^+$ ($pK_b$~6.5–9) and $COO^-$ ($pK_a$~3–4) or $OSO_3^-$ ($pK_a$~2) moieties. Under more acidic conditions, an insufficient ionization of the anionic polyelectrolytes leads to a substantial decrease in the number of interactions established with the precursor cations, resulting in the destabilization of the PEC. In the case of CS/XG-based PECs, however, this destabilization is not observed. Though electrostatic interactions between the $NH_3^+$ moieties of CS and $COO^-$ groups of XG play a significant role, additional interactions such as hydrogen bonding have been described as crucial for PEC production as well, as discussed above. This feature represents an additional advantage in the interaction with the polycation, leading to the production of PECs which are stable in a wider pH window.

### 3.2. CS-XG PEC-based aerogel

The CS-XG (1%) PECs led to stable aerogels, but the samples shrank substantially after the supercritical process. The effect of the $scCO_2$-drying conditions on the generated materials was evaluated. The materials obtained at the processing pressures of 150 bar and 250 bar are shown in Fig. 3. Both aerogels present whitish, bone-like structures and possess similar macroscopic characteristics, showing no evidence for the modification of the pore network and/or scattering of the polymer.

The texture and structure of the cryogels produced from the other polyelectrolyte combinations tested were macroscopically very different when compared to the CS-XG (1%) aerogels, originating either whitish sponge-like (the XG-derived cryogels) or foam-like (the remaining cryogels obtained) materials after freeze-drying.

#### 3.2.1. Physical characterization

The aerogels produced at different drying conditions from the CS-XG (1%) PEC (CX9 samples) were characterized. The corresponding cryogel was also studied and comparatively assessed. Fig. 4 shows the SEM images of the inner part of the CS-XG (1%) aerogels and cryogel, at 25 000 × amplification. Consistently with the macroscopic views, the SEM microphotographs reveal no significant differences in the microstructure of the CS-XG aerogels obtained at 150 and 250 bar, but substantial changes as far as the cryogel is concerned. Indeed, while the cryogel presents a granular-like structure and a rough surface, the aerogels show a dense and smooth surface. The degree of roughness decreases from micro to nano-scale level when comparing the cryogels and aerogels, respectively. In both cases, however, a three-dimensional porous network is not visible below 25 000 × amplification, being the distribution of the pores irregular.

Nitrogen adsorption technique enabled to obtain the pore size distribution as well as the BET surface area. Fig. 5 displays the data gathered for the CX9 sample. All the materials present (very similar) Type II isotherms, suggesting *a priori* a non-porous structure or macroporosity, according to the IUPAC classification [46]. The porosity values (Table 2) obtained from the adsorption isotherms, show pore sizes in the mesopore range, being the average pore diameter of aerogels (~20 nm) remarkably higher than that of the cryogel (~4 nm). No significant difference is observed in the average pore diameter of the aerogels obtained at these two conditions. Fig. 5A shows uniform distributions of pore sizes extending from 5 to 75 nm in the case of the aerogels, and a slightly narrower pore distribution (30–65 nm) corresponding to the cryogel. Both aerogels and the cryogel have mostly pores in the mesopore region (~60–70% and ~80%, respectively), as reported for numerous aerogels with well-developed uniform mesoporosity [47]. Micro and macroporosity are observed as well to a similar extent. The aerogel processed at 250 bar exhibits the largest specific surface area (~18 $m^2\ g^{-1}$), while the aerogel dried at 150 bar and the cryogel present significantly lower surface area values. In both cases, the depressurization rate was 5 bar/min, which means that the values of this property are determined by the intrinsic characteristics of the aerogel materials. The specific surface areas of the materials under study are below the data commonly reported for aerogels (500–1200 $m^2\ g^{-1}$) [3].

The values of the density obtained by helium picnometry are given in Table 2. The aerogel produced at 250 bar presents the lowest density, while the other two materials exhibit higher and closer values. This suggests compaction of the sample when it is processed at higher $CO_2$ pressure. The aerogels obtained in this work have larger densities than

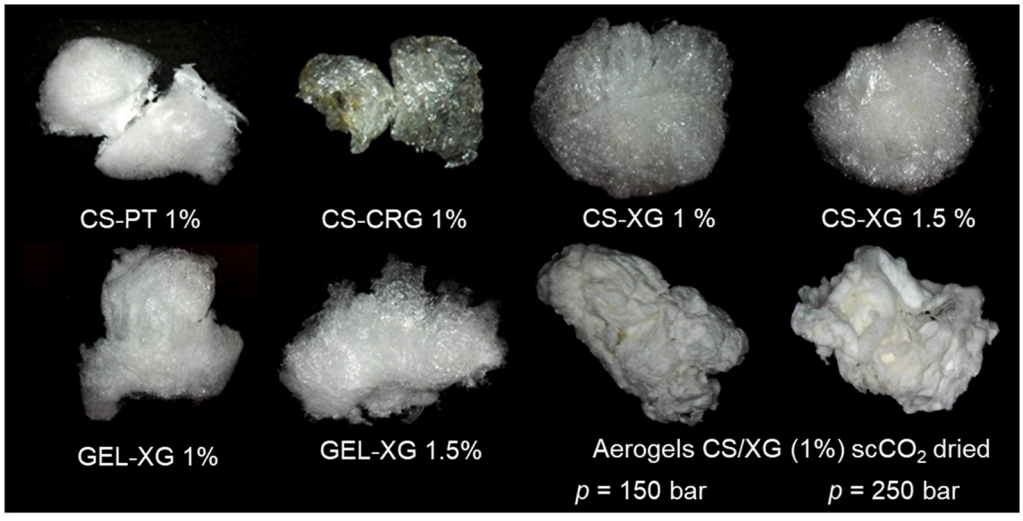


**Fig. 3.** Cryogels obtained from the chitosan-based PECs, and aerogels obtained from the CS/XG PEC, at two different sc-drying conditions: 35 °C, 4 h, q = 0.5 ml/min.

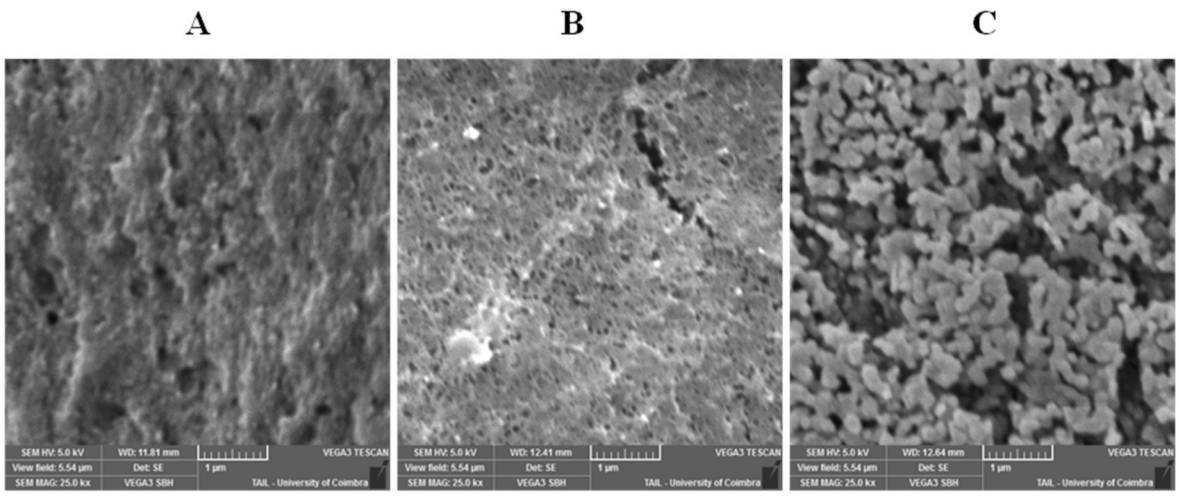


**Fig. 4.** Scanning electron microscopy images of the cross-section of the CS/XG aerogels $scCO_2$-dried at 150 bar (**A**) and at 250 bar (**B**).

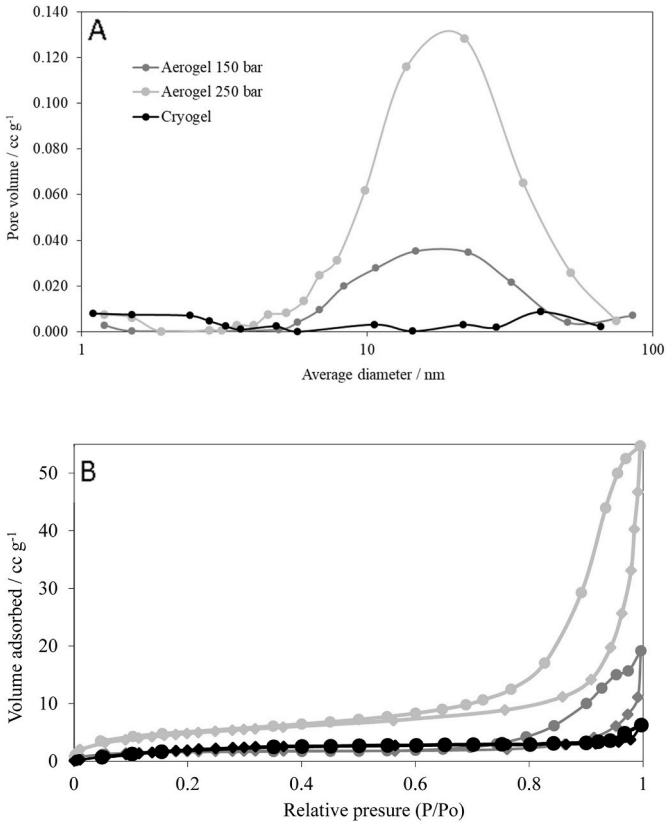


**Fig. 5.** Nitrogen adsorption isotherms for the CS-XG aerogels $scCO_2$-dried at 150 bar (dark grey) and at 250 bar (light grey), and for the cryogels (black). Adsorption (—◆—), desorption (—•—) **(A)**.BJH pore size distribution for the CS-XG 1% aerogels and cryogel, derived from the nitrogen desorption isotherms **(B)**.

the decimal values usually reported in the literature [3]. As far as we are aware, there is no data available in the literature for the physicochemical properties of CS-XG-based aerogels.

In Table 2, the data gathered by mercury intrusion porosimetry is summarized. The CS-XG-based materials have porosities between 60 and 85%. The aerogels present lower porosities than the cryogel. The porosity obtained for the aerogel processed at 150 bar is higher than when it is dried at 250 bar. The porous structure of the cryogel confers a lower bulk density since air occupies the free space present in this 85% porous material. Yet, the main difference observed between the aerogels and the cryogel is in the total pore area (~20–40 times higher for the aerogels). Indeed, the lyophilization process leads to larger pores, and larger pores result in smaller areas. Comparing the physical properties of the aerogels processed at different conditions, the aerogel produced at 150 bar shows higher porosity and, consistently, lower densities.

In face of the data summarized in Table 2, the CS-XG-aerogels and cryogel should have mesopores in the range of 5–20 nm, and macropores between 0.2 and 35 µm, with the aerogels having larger mesopores and significantly narrower macropores than the cryogel. The aerogel $scCO_2$-dried at 150 bar shows the highest porosity and the lowest densities, being closer to the desirable characteristics of an aerogel. In face of these results, it can be potentially used in the environmental area, as an adsorbent in wastewater treatment, or for tissue engineering applications as cutaneous wound dressings. Their application as scaffolds for bone regeneration should be pondered as well, though further studies are needed.

The applications of CS-XG systems have been mostly studied in the form of hydrogels, for the encapsulation and controlled release of food ingredients, cells, enzymes and therapeutic agents and dermal dressings [40]. Establishing applications of the CS-XG hydrogels produced in this work requires further studies, out of the scope of the current paper. Nevertheless, the evidence obtained for PEC formation leaves this possibility open.

It would be also important to point out that the interesting characteristics presented by the XG-based cryogels confer potential for a variety of applications in distinct areas. Indeed, their distinct features when compared to the aerogels, namely the roughness and sponge-like appearance, as well as a higher porosity, lower densities, smaller mesopores and remarkably larger macropores, are promising for valuable uses. A high degree of roughness can enable the dissociation of drug molecules in drug release applications, whereas a higher porosity can represent an advantage as far as bone regeneration is concerned. The cryogels are therefore good candidates for cutaneous wound dressings and their application as scaffolds should be considered as well. For biomedical applications, a porosity of at least 80% is recommended, which only happens with the cryogel.

It is worth noticing that the presence of the CS component confers an additional advantage to the materials developed in this work, due to the well-established dermal and healing properties of this natural polyelectrolyte [11].

Finally, the PECs which did not provide aerogels do still have potential applications in the field of ecology, biotechnology, medicine and pharmaceutical technology. Samples of CS-PT and CS-CRG PECs can be applied in regenerative medicine, after going through an appropriate

**Table 2**
Physical characterization of the CS-XG (1%) aerogels and cryogel samples.

| Processing Conditions | Nitrogen adsorption | | Helium pycnometry | Mercury intrusion porosimetry | | | |
|---|---|---|---|---|---|---|---|
| | Pore diameter (nm) | Specific surface area (BET) ($m^2.g^{-1}$) | Real density (g. $cm^{-3}$) | Bulk density (g. $cm^{-3}$) | Porosity (%) | Total pore area ($m^2.g^{-1}$) | Pore diameter (nm) |
| **$scCO_2$-dried at 150 bar** | 2.1–261.2 | 5.7 ± 0.2 | 1.3 ± 0.3 | 0.24 | 67.93 | 22.07 | 0.007–169.2 |
| **$scCO_2$-dried at 250 bar** | 2.2–259.1 | 17.5 ± 0.4 | 1.21 ± 0.04 | 0.36 | 59.72 | 38.82 | 0.007–169.1 |
| **Freeze-dried** | 2.3–101.1 | 9.1 ± 0.3 | 1.26 ± 0.07 | 0.099 | 84.94 | 0.997 | 0.007–171.3 |

sterilization process.

For the applications suggested in this work, particularly as far as the biomedical area is concerned, the production of cytotoxicity data of the material is highly desirable. This is out of the scope of the present work but proposed for further investigation.

### 3.2.2. Thermal analysis

Fig. 6 shows the SDT thermogravimetric and calorimetric profile of CS-XG 1% aerogels and cryogel samples, and Table 3 summarizes the temperature of the thermal events observed, as well as the mass losses determined for the materials.

Globally speaking, all the DTG curves show two events, being the first indicative of a first degradation step and the second one suggestive of further thermal decomposition of the materials. These events are coincident with the two exothermic peaks of the calorimetric curve and are thus correspondent to the referred events. These data suggest that the thermal degradation pattern of the materials occurs in two steps which are likely to be attributed to a successive degradation of XG and CS, since the initial decomposition temperature of these polymers has been reported as 266 °C and 293 °C, respectively, occurring in the range 250–330 °C for XG and 283-360 °C for CS [48]. Furthermore, the DSC thermograms of the polysaccharides show major intense peaks around 300 °C, followed or preceded by weaker exotherms [48].

The first event of the DTG curve of both the aerogels is located around 240 °C and the second around 300 °C, being the temperature observed for the aerogel processed at 150 bar higher than that of the aerogels dried at 250 bar (Table 3). The values of the temperature obtained from SDT analysis for the first and second events in the case of the cryogel are lower. The same trend is observed for corresponding calorimetric data, except for the second calorimetric event of the cryogel, which occurs at a higher temperature.

The aerogels are thermally stable up to ~240 °C, while the cryogel is thermally stable up to a lower temperature value of ~224 °C. The value of the total weight loss through thermal decomposition of the aerogels (~25%) is smaller than that of the cryogel (~40%). The mass loss of the polysaccharides precursors was found to be near 50% [48], meaning that the association of the polymers results in more thermally stable materials, particularly as far as the aerogels are concerned.

**Table 3**
Temperature of thermal events obtained from SDT analysis of the CS-XG 1% aerogels and cryogel.

| Processing Conditions | Thermogravimetric data (SDT, °C) | | Calorimetric data (°C) | | Mass loss (%) | |
|---|---|---|---|---|---|---|
| | 1st event | 2nd event | 1st event | 2nd event | 1st event | 2nd event |
| **$sc-CO_2$ dried at 150 bar** | 240.0 ± 0.59 | 301.0 ± 1.4 | 234.5 ± 2.2 | 276.4 ± 1.15 | 13.8 ± 0.11 | 10.5 ± 0.84 |
| **$sc-CO_2$ dried at 250 bar** | 238.0 ± 1.7 | 288.6 ± 2.3 | 239.7 ± 2.8 | 275.1 ± 0.16 | 13.4 ± 0.56 | 11.5 ± 0.64 |
| **Freeze-dried** | 224.4 ± 1.4 | 279.9 ± 1.2 | 212.8 ± 0.02 | 287.9 ± 0.26 | 11.4 ± 0.80 | 26.8 ± 0.53 |

## 4. Conclusion

A novel aerogel was obtained from a chitosan-xanthan gum polyelectrolyte complex (PEC), after the screening of thirteen different combinations of natural polyelectrolytes.

Among the combinations tested, PEC formation was visually detected for eight systems and additionally corroborated by FTIR evidence only for the CS-PT, CS-CRG and CS-XG PECs. It has been shown that only the CS-XG PECs prepared from 1% (m/v) starting solutions yielded aerogels by $scCO_2$-drying, while all systems provided stable cryogels.

The morphology, structure and properties of the CS-XG (1%) materials obtained at two $scCO_2$-drying conditions as well as of the corresponding cryogel were elucidated by various physicochemical techniques. The CS-XG aerogels have bone-like structures and smooth

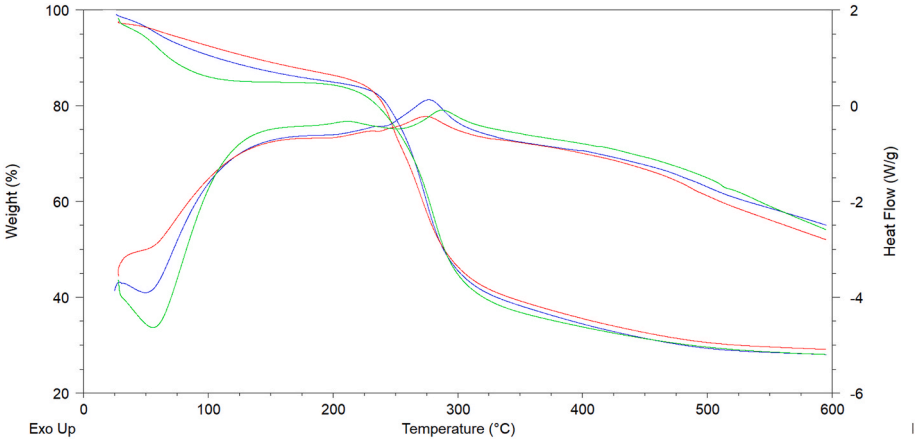


**Fig. 6.** SDT thermograms of the CS-XG 1% aerogel dried at 150 bar (blue) and at 250 bar (red), and of the cryogel (green). (For interpretation of the references to colour in this figure legend, the reader is referred to the Web version of this article.)

surfaces, while the cryogel has a sponge-like structure and rough surface. The distribution of the pore sizes of the materials is mostly in the meso and macropore ranges, being the porosity of the cryogel of about 85%, and higher than that of the aerogels. The aerogels present larger mesopores and significantly smaller macropores than the cryogel. The aerogel processed at 150 bar shows higher porosity and, consistently, lower densities than the aerogel produced at 250 bar.

The thermal analysis shows that the aerogels are thermally stable up to a higher temperature than the cryogel and suffer considerably less mass loss through thermal decomposition.

In face of the properties shown, the CS-XG-based aerogels developed are promising candidates for environmental and tissue engineering applications, namely as adsorbents for wastewater treatment, as cutaneous wound dressings and eventually as scaffolds for bone regeneration.

## CRediT authorship contribution statement

**Luciana I.N. Tomé:** Methodology, Investigation, Writing – original draft, preparation. **Marco S. Reis:** Methodology, Validation, Writing – review & editing. **Hermínio C. de Sousa:** Conceptualization, Writing – review & editing. **Mara E.M. Braga:** Funding acquisition, Project administration, Supervision, Conceptualization, Writing – review & editing.

## Declaration of competing interest

The authors declare that they have no known competing financial interests or personal relationships that could have appeared to influence the work reported in this paper.

## Acknowledgements

This work was financially supported by Fundação para a Ciência e Tecnologia (FCT), Portugal, through the project STERILAEROGEL – Green method to prepare sterilised biopolymer-based aerogel (POCI-01-0145-FEDER-032625), Strategic Projects FCT-MEC PEst-C/EQB/UI0102/2019 and UIDB/04539/2020, and Projects UIDB/00102/2020 and UIDP/00102/2020 (CIEPQPF). The authors also acknowledge Professor Marta R. Fontanilla (Universidad Nacional de Colombia) for the supply of the collagen samples.

## Appendix A. Supplementary data

Supplementary data to this article can be found online at https://doi.org/10.1016/j.matchemphys.2022.126294.

## References

[1] C.A. García-González, T. Budtova, L. Durães, C. Erkey, P. Del Gaudio, P. Gurikov, M. Koebel, F. Liebner, M. Neagu, I. Smirnova, An opinion paper on aerogels for biomedical and environmental applications, Molecules 24 (2019) 1815–1831.
[2] L. Zheng, S. Zhang, Z. Ying, J. Liu, Y. Zhou, F. Chen, Engineering of aerogel-based biomaterials for biomedical applications, Int. J. Nanomed. 15 (2020) 2363–2378.
[3] H. Maleki, L. Durães, C.A. García-González, P. del Gaudio, A. Portugal, M. Mahmoudi, Synthesis and biomedical applications of aerogels: possibilities and challenges, Adv. Colloid Interface Sci. 236 (2016) 1–27.
[4] F.P. Soorbaghi, M. Isanejad, S. Salatin, M. Ghorbani, S. Jafari, H. Derakhshankhah, Bioaerogels: synthesis approaches, cellular uptake, and the biomedical applications, Biomed, Pharma 111 (2019) 964–975.
[5] S. Zhao, W.J. Malfait, N. Guerrero-Alburquerque, M.M. Koebel, G. Nystrom, Biopolymer aerogels and foams: chemistry, properties, and applications, Angew. Chem. Int. Ed. 57 (2018) 7580–7608.
[6] G. Thakur, F.C. Rodrigues, K. Singh, Crosslinking biopolymers for advanced drug delivery and tissue engineering applications, in: H.J. Chun (Ed.), Advances in Experimental Medicine and Biology, Springer Nature, Singapore, 2018 (Chapter 11).
[7] S.L. Orellana, A. Giacaman, A. Vidal, C. Morales, F. Oyarzun-Ampuero, J.G. Lisoni, C. Henriquez-Baez, L. Moran-Trujillo, M. Concha, I. Moreno-Villoslada, Chitosan/chondroitin sulfate aerogels with high polymeric electroneutralization degree: formation and mechanical properties, Pure Appl. Chem. 90 (2018) 901–911.
[8] S. Takeshita, S. Zhao, W.J. Malfait, Transparent, aldehyde-free chitosan aerogel, Carbohydr. Polym. 251 (2021) 117089–117097.
[9] L.E. Nita, A. Ghilan, A.G. Rusu, I. Neamtu, A.P. Chiriac, New trends in bio-based aerogels, Pharmaceutics 12 (2020) 449–480.
[10] A.D. Kulkarni, Y.H. Vanjari, K.H. Sancheti, H.M. Patel, V.S. Belgamwar, S. J. Surana, C.V. Pardeshi, Polyelectrolyte complexes: mechanisms, critical experimental aspects, and applications, Artif. Cells Nanomed, Biotechnol. 44 (2016) 1615–1625.
[11] M. Ishihara, S. Kishimoto, S. Nakamura, Y. Sato, H. Hattori, Polyelectrolyte complexes of natural polymers and their biomedical applications, Polymers 11 (2019) 672–684.
[12] J. Berger, M. Reist, J.M. Mayer, O. Felt, N.A. Peppas, R. Gurny, Structure and interactions in covalently and ionically crosslinked chitosan hydrogels for biomedical applications, Eur. J. Pharm. Biopharm. 57 (2004) 19–34.
[13] K. Ganesan, T. Budtova, L. Ratke, P. Gurikov, V. Baudron, I. Preibisch, P. Niemeyer, I. Smirnova, B. Milow, Review on the production of polysaccharide aerogel particles, Materials 11 (2018) 2144–2181.
[14] S. Wei, Y.C. Ching, C.H. Chuah, Synthesis of chitosan aerogels as promising carriers for drug delivery: a review, Carbohydr. Polym. 231 (2020) 115744–115757.
[15] D.A.S. Agostinho, A.I. Paninho, T. Cordeiro, A.V.M. Nunes, I.M. Fonseca, C. Pereira, A. Matias, M.G. Ventura, Properties of κ-carrageenan aerogels prepared by using different dissolution media and its application as drug delivery systems, Mater. Chem. Phys. 253 (2020) 123290–123301.
[16] K. Rinki, P.K. Dutta, A.J. Hunt, D.J. Macquarrie, J.H. Clark, Chitosan aerogels exhibiting high surface area for biomedical application: preparation, characterization, and antibacterial study, Int. J. Polym. Mater. 60 (2011) 988–999.
[17] K. Ganesan, L. Ratke, Facile preparation of monolithic k-carrageenan aerogels, Soft Matter 10 (2014) 3218–3224.
[18] S. Groult, T. Budtova, Tuning structure and properties of pectin aerogels, Eur. Polym. J. 108 (2018) 250–261.
[19] C.A. García-González, M. Alnaief, I. Smirnova, Polysaccharide-based aerogels-promising biodegradable carriers for drug delivery systems, Carbohydr. Polym. 86 (2011) 1425–1438.
[20] [a] D.A.S. Agostinho, A.I. Paninho, T. Cordeiro, A.V.M. Nunes, I.M. Fonseca, C. Pereira, A. Matias, M.G. Ventura, Properties of k-carrageenan aerogels prepared by using diferente dissolution media and its application as drug delivery system, Mater. Chem. Phys. 253 (2020) 123290–123301;
[b] M.P. Batista, V.S.S. Gonçalves, F.B. Gaspar, I.D. Nogueira, A.A. Matias, P. Gurikov, Novel alginate-chitosan aerogel fibres for potential wound healing applications, Int. J. Biol. Macromol. 156 (2020) 773–782.
[21] G. Horvat, K. Xhanari, M. Finsgar, L. Gradisnik, U. Maver, Z. Knez, Z. Novak, Novel ethanol-induced pectin–xanthan aerogel coatings for orthopedic applications, Carbohydr. Polym. 166 (2017) 365–376.
[22] M. Pantic, G. Horvat, Z. Knez, Z. Novak, Preparation and characterization of chitosan-coated pectin aerogels: curcumin case study, Molecules 25 (2020) 1187–1202.
[23] M. Martins, A.A. Barros, S. Quraishi, P. Gurikov, S.P. Raman, I. Smirnova, A.R. C. Duarte, R.L. Reis, Preparation of macroporous alginate-based aerogels for biomedical applications, J. Supercrit. Fluids 106 (2015) 152–159.
[24] S. Khan, M. Ul-Islam, M. Ikram, S.U. Islam, M.W. Ullah, M. Israr, J.H. Jang, S. Yoon, J.K. Park, Preparation and structural characterization of surface modified microporous bacterial cellulose scaffolds: a potential material for skin regeneration applications *in vitro* and *in vivo*, Int. J. Biol. Macromol. 117 (2018) 1200–1210.
[25] A. Muñoz-Ruíz, D.M. Escobar-García, M. Quintana, A. Pozos-Guillén, H. Flores, Synthesis and characterization of a new collagen-alginate aerogel for tissue engineering, J. Nanomater. (2019) 10, https://doi.org/10.1155/2019/2875375, 2875375.
[26] N.A. Valchuk, O.S. Brovko, I.A. Palamarchuk, T.A. Boitsovaa, K.G. Bogolitsyn, A. D. Ivakhnov, D.G. Chukhchin, N.I. Bogdanovich, Preparation of aerogel materials based on alginate-chitosan interpolymer complex using supercritical fluids, Russ. J. Phys. Chem. B 13 (2019) 1121–1124.
[27] G. Della Porta, P. Del Gaudio, F. De Cicco, R.P. Aquino, E. Reverchon, Supercritical drying of alginate beads for the development of aerogel biomaterials: optimization of process parameters and exchange solvents, Ind. Eng. Chem. Res. 52 (2013) 12003–12009.
[28] L. Baldino, S. Cardea, E. Reverchon, Natural aerogels production by supercritical gel drying, Chem. Eng. Trans. 43 (2015) 739–744.
[29] E. Suesca, A.M.A. Dias, M.E.M. Braga, H.C. de Sousa, M.R. Fontanilla, Multifactor analysis on the effect of collagen concentration, cross-linking and fiber/pore orientation on chemical, microstructural, mechanical and biological properties of collagen type I scaffolds, Mater. Sci. Eng. C 77 (2017) 333–341.
[30] I.J. Seabra, M.E.M. Braga, H.C. de Sousa, Statistical mixture design investigation of $CO_2$-ethanol-$H_2O$ pressurized solvent extractions from tara seed coat, J. Supercrit. Fluids 64 (2012) 9–18.
[31] K.L.B. Chang, G. Tsai, J. Lee, W.-R. Fu, Heterogeneous N-deacetylation of chitin in alkaline solution, Carbohydr. Res. 303 (1997) 327–332.
[32] M. Lavertu, Z. Xia, A.N. Serreqi, M. Berrada, A. Rodrigues, D. Wang, M. D. Buschmann, A. Gupta, A validated 1H NMR method for the determination of the degree of deacetylation of chitosan, J. Pharmaceut. Biomed. Anal. 32 (2003) 1149–1158.
[33] A. Baxter, M. Dillon, K.D. Taylor, G.A.F. Roberts, Improved method for i.r. determination of the degree of N-acetylation of chitosan, Int. J. Biol. Macromol. 14 (1992) 166–169.
[34] M.R. Sierakowski, M. Milas, J. Desbrières, M. Rinaudo, Specific modifications of galactomannans, Carbohydr. Polym. 42 (2000) 51–57.

[35] C. Li, S. Hein, K. Wang, Chitosan-carrageenan polyelectrolyte complex for the delivery of protein drugs, ISRN Biomater. 6 (2013) 1–6.
[36] J.E. McBane, B. Vulesevic, D.T. Padavan, K.A. McEwan, G.S. Korbutt, E. J. Suuronen, Evaluation of a collagen-chitosan hydrogel for potential use as a pro-angiogenic site for islet transplantation, PLoS One 8 (2013), e77538.
[37] B. Kaczmarek, A. Sionkowska, J. Stojkovska, Characterization of scaffolds based on chitosan and collagen with glycosaminoglycans and sodium alginate addition, Polym. Test. 68 (2018) 229–232.
[38] E.V. Shumilina, Yu A. Shchipunov, Chitosan–carrageenan gels, Colloid J. 64 (2002) 372–378.
[39] C. Deka, M. Dutta, D. Deka, D.K. Jha, D.K. Kakati, Study of olive oil-loaded chitosan/carrageenan coacervate and its antibacterial property, Int. J. Pharma Sci. 6 (2016) 1524–1533.
[40] S. Argin-Soysal, P. Kofinas, Y.M. Lo, Effect of complexation conditions on xanthan–chitosan polyelectrolyte complex gels, Food Hydrocolloids 23 (2009) 202–209.
[41] Y. Benjamini, Y. Hochberg, Controlling the false discovery rate: a practical and powerful approach to multiple testing, J. Roy. Stat. Soc. B 57 (1995) 289–300.
[42] N. Al-Zebari, S.M. Best, R.E. Cameron, Effects of reaction pH on self-crosslinked chitosan-carrageenan polyelectrolyte complex gels and sponges, J. Phys.: Materials 2 (2019), 01500.
[43] A.J. Martinéz-Goméz, L.E. Cruz-Barba, J.C. Sanchéz-Díaz, F. Becerra-Bracamontes, A. Martinéz-Ruvalcaba, Plasma enhanced modification of xanthan and its use in chitosan/xanthan hydrogels, Polym. Eng. Sci. (2014) 2264–2271.
[44] M.N. Taravel, A. Domard, Collagen and its interaction with chitosan II. Influence of the physicochemical characteristics of collagen, Biomaterials 16 (1995) 865–871.
[45] C. Lii, S.C. Liaw, V.M.-F. Lai, P. Tomasik, Xanthan gum-gelatin complexes, Eur. Polym. J. 38 (2002), 1377-1371.
[46] J. Rouquerol, D. Avnir, C.W. Fairbridge, D.H. Everett, J.M. Haynes, N. Pernicone, J. D.F. Ramsay, K.S.W. Sing, K.K. Unger, Recommendations for the characterization of porous solids (Technical Report), Pure Appl. Chem. 66 (1994) 1739–1758.
[47] I. Smirnova, P. Gurikov, Aerogels in chemical engineering: strategies toward tailor-made aerogels, Annu. Rev. Chem. Biomol. Eng. 8 (2017) 307–334.
[48] M.J. Zohuriaan, F. Shokrolahi, Thermal studies on natural and modified gums, Polym. Test. 23 (2004) 575–579.